

Up-Regulation of Glis2 Involves in Neuronal Apoptosis After Intracerebral Hemorrhage in Adult Rats

Kaifu Ke · Yan Song · Jiabing Shen · Mu Niu ·
Haiyan Zhang · Daming Yuan · Haidan Ni ·
Yu Zhang · Xiaorong Liu · Aihua Dai · Maohong Cao

Received: 1 September 2014 / Accepted: 24 October 2014 / Published online: 5 November 2014
© Springer Science+Business Media New York 2014

Abstract The novel Krüppel-like zinc finger protein Gli-similar 2 (Glis2), one member of the transcription factors, is involved in controlling the flow of genetic information and the modulation of diverse cellular activities. Accumulating evidence has demonstrated its important roles in adult development and several diseases. However, information regarding the regulation and possible function of Glis2 in the central nervous system is still limited. In this study, we explored the roles of Glis2 during the pathophysiological process of intracerebral hemorrhage (ICH). An ICH rat model was established and assessed by behavioral tests. Expression of Glis2 was significantly up-regulated in brain areas surrounding the hematoma following ICH. Immunofluorescence showed that Glis2 was strikingly increased in neurons, but not astrocytes or microglia. Up-regulation of Glis2 was found to be accompanied by the increased expression of active caspase-3 and Bax and decreased expression of Bcl-2 in vivo and vitro studies. Moreover, knocking down Glis2 by RNA-interference in PC12 cells reduced active caspase-3 and Bax expression while increased Bcl-2. Collectively, we speculated that Glis2 might exert pro-apoptotic function in neurons following ICH.

Keywords Intracerebral hemorrhage · Glis2 · Neuronal apoptosis · Rat

Introduction

Intracerebral hemorrhage (ICH), acute and spontaneous rupture of blood vessels in the brain, is the second most common subtype of stroke with high morbidity and mortality (Hwang et al. 2011; Ikram et al. 2012). Till now, lots of resources have been invested into clinical and basic researches regarding ICH, but the clinical outcome remains poor (Ikram et al. 2012). Rupture of blood vessels within brain parenchyma leads to primary and secondary injuries. Primary injury comes from the mass effect of hematoma formation and compression. Secondary injury is for the most part due to the presence of intraparenchymal blood, which subsequently activates oxidative, cytotoxic, and inflammatory pathways. This pathogenesis ultimately leads to irreversible disruption of the components of the neurovascular unit, blood–brain barrier disruption and massive brain cell death (Keep et al. 2012; Aronowski and Zhao 2011). Among them, neuronal apoptosis is regarded as one of the most crucial events and it can be divided into extrinsic pathway and intrinsic pathway. The former is triggered by the ligation of death receptors and recruitment and activation of caspase-8. The latter depends on mitochondria-mediated apoptosis pathway. Up-regulation of pro-apoptotic Bcl-2-associated X protein (Bax) levels and concurrent down-regulation of anti-apoptotic protein B cell lymphoma-2 (Bcl-2) facilitate release of cytochrome c and activation of caspases and eventually result in cell apoptosis (Plesnila et al. 2007; Cregan et al. 1999; Wu et al. 2012). Caspase-3 is the predominant executioner and can be frequently activated during both pathways (Elmore

Kaifu Ke and Yan Song contributed equally to this work.

K. Ke · Y. Song · J. Shen · M. Niu · H. Zhang · D. Yuan ·
H. Ni · Y. Zhang · X. Liu · A. Dai · M. Cao (✉)
Department of Neurology, Affiliated Hospital of Nantong
University, Nantong 226001, Jiangsu Province,
People's Republic of China
e-mail: cmhongnt@sina.com

Y. Song · J. Shen · M. Niu
Jiangsu Province Key Laboratory for Inflammation
and Molecular Drug Target, Nantong University,
Nantong 226001, Jiangsu Province, People's Republic of China

2007). Although a lot of studies have revealed the biological process of ICH, definite mechanisms of neuronal apoptosis under this issue are not fully understood.

Krüppel-like zinc finger proteins constitute one of the biggest families of transcription factors, which have important regulatory functions during development and have also been implicated in a variety of diseases (Zhang and Jetten 2001; Villavicencio et al. 2000). Gli-similar 2 (Glis2), as one member of Krüppel-like zinc finger transcription factors, is a relatively proline-rich, basic 55.8 kDa protein (Zhang et al. 2002). Feng Zhang has demonstrated that Glis2 mRNA was expressed in several adult tissues, including kidney, lung, heart, and brain through Northern blot analysis (Zhang and Jetten 2001). Glis2 was also expressed in the cranial and dorsal ganglia, the neural tube, and in the intermediate zones of the hindbrains of mouse embryos (embryonic day 9.5), promoting the differentiation of neuronal precursor cells (Kim et al. 2008). Previous studies have revealed that mice deficient in Glis2 would like to develop progressive tubular atrophy, glomerulosclerosis, renal failure, and premature death (Vasanth et al. 2011; Attanasio et al. 2007). Changes of gene expression in kidney in Glis2^{mut} mice included kinds of apoptosis-related factors, such as members of Bcl-2 family (Kim et al. 2008). As Glis2 has been reported to be expressed in neurons and involved in cell death, we tried to explore the expression and possible function of Glis2 in the brain during ICH. It was found that Glis2 was up-regulated around the hematoma and involved in neuronal apoptosis. Our research was conducted to gain greater insight into the functions of Glis2 in the CNS, further making appropriate suggestions for clinical trials.

Materials and Methods

Animals and the ICH Model

Male Sprague–Dawley rats (220–250 g) provided by the Department of Animal Center, Medical College of Nantong University were used in this study. They were kept in a temperature-controlled environment (21 °C) on a 12 h light–dark cycle. Rats were anesthetized intraperitoneally with sodium pentobarbital (50 mg/kg) positioned in a stereotaxic frame, and a cranial burr hole (1 mm in diameter) was drilled near the right coronal suture 3.5 mm lateral to the midline. Autologous whole blood (50 µL) was collected from its tail tip and was collected in a sterile syringe. The sterile syringe was inserted stereotactically into the right basal ganglia (coordinates: 0.2 mm anterior, 5.5 mm ventral, and 3.5 mm lateral to the bregma) (Yang et al. 2008; Li et al. 2013). The autologous blood was injected at the rate of 10 µL/min. 10 min later, the needle was

removed, the skin incision closed, and the animals were allowed to recover. Sham-controlled rats received an equivalent volume of saline. Experimental animals ($n = 8$ per time point) were sacrificed to extract the protein for Western blot analysis at 6 and 12 h, 1, 2, 3, 5, 7, and 9 days after ICH, respectively. The sham-operated animals ($n = 8$ per time point) were sacrificed on the second day. Additional experimental animals at each time point were killed for pathologic studies. Experiments were carried out in accordance with the National Institutes of Health (NIH) Guidelines for the Care and Use of Laboratory and approved by the Chinese National Committee to Use of Experimental Animals for Medical Purposes, Jiangsu Branch. All efforts were made to minimize the number of animals used and suffering.

Behavioral Testing Procedures

Forelimb placing and corner turn tests were used to assess the neurological deficits induced by ICH.

Forelimb Placing Test

Forelimb placing test was performed as described (Karabiyikoglu et al. 2004). The rats were held by torsos, allowing the forelimb to hang free. Testing of each forelimb was performed by brushing the vibrissae on the corner edge of a countertop. Intact rats placed the forelimb quickly onto the countertop. According to the severity of injury, placing of the forelimb contralateral to the injury was impaired. During the experiments, every rat was tested 10 times for each forelimb. The percentage of trials in which the rat placed its left forelimb was calculated.

Corner Turn Test

Corner turn test was performed as described (Li et al. 2013). Rats proceed into a corner, whose angle was 30°. In order to exit the corner, the rats should turn to the left or the right, only the turns involving full rearing along either wall were involved (a total of eight per animal). Injured rats would show a tendency to turn to the side of the injury. The percentage of right turns was used as the corner turn score. After each turn, the rats were not picked up immediately, so that they would not develop an aversion for their prepotent turning response.

Cell Cultures and Stimulation

Rat pheochromocytoma (PC12) cells were obtained from the American Type Culture Collection (Rockville, MD) and were cultured in Dulbecco's modified Eagle's medium (DMEM) supplemented with 10 % (v/v) fetal bovine serum

and 1 % penicillin/streptomycin at 37 °C under 5 % CO₂ and 95 % oxygen in humidified air. The medium was changed every 2 days. In order to study apoptosis, PC12 cells were seeded onto 60-mm dishes and incubated in a low concentration of serum (1 % horse serum) for 24 h prior to treatment with hemin (100 µmol/L) for different time points.

siRNAs and Transfection

The DNA target sequence for the rat Glis2 (NM_001106978.1) gene was GCAAGAGAGAAGCGAGAAATT. For transient transfection, the siRNA vector and the nonspecific vector were carried out using lipofectamine 2000 (Invitrogen) and plus reagent basic DMEM (serum free) according to the manufacturer's instructions. Transfected cells were used for the subsequent experiments 48 h after transfection.

Western Blot Analysis

Rats were sacrificed at 6 and 12 h, 1, 2, 3, 5, 7, and 9 days after operation. Brain tissues surrounding the hematoma (extending 2 mm from the boundary of hematoma) and the counterparts from the contralateral side of the brain or the sham-operated group were dissected and flash-frozen at –80 °C until use. In order to prepare lysates, frozen samples were weighed and minced on ice. Then, the tissues were homogenized in lysis buffer (1 % NP-40, 50 mmol/L Tris, 1 % SDS, 5 mmol/L EDTA, 1 % sodium deoxycholate, 1 % Triton-X100, 1 mmol/L PMSF, 10 µg/mL aprotinin, and 1 µg/mL leupeptin, pH = 7.5) and centrifuged at 12,000 rpm at 4 °C for 20 min to collect the supernatant. The resulting supernatant was subjected to SDS–polyacrylamide gel electrophoresis (PAGE) and transferred to polyvinylidene difluoride filter membranes (PVDF) by a transfer apparatus after determining the protein concentration with the Bradford assay (Bio-Rad). The membranes were blocked with 5 % non-fat milk for 2 h and incubated with primary antibody against Glis2 (anti-goat, 1:200, Santa Cruz), Bax (anti-rabbit, 1:500, Santa Cruz), Bcl-2 (anti-mouse, 1:500, Santa Cruz), active caspase-3 (anti-mouse, 1:500, Cell Signaling), and GAPDH (anti-rabbit, 1:1,000, Sigma). At last, the membranes were incubated with secondary antibodies for 2 h and visualized with an enhanced chemiluminescence (ECL) kit (Pierce) or scanned with the Odyssey Infrared Imaging System (LI-COR Bioscience).

Sections and Immunocytochemical

Rats 2 days after ICH and from the sham-operated group ($n = 3$ each group) were anesthetized with chloral hydrate

(10 % solution) and perfused pericardially with 0.9 % saline followed by 4 % paraformaldehyde. After perfusion, brains were removed, post-fixed in the same fixative for 1 day at room temperature (RT), and subsequently soaked in 20 and 30 % sucrose for 2–3 days, respectively. After that, the brain tissues were cut at 4 µm with a cryostat and then stored at –20 °C until use for immunohistochemistry and immunofluorescence.

For immunohistochemistry, brain sections were firstly washed in PBS and then blocked with 3 % H₂O₂ for 30 min at room temperature to reduce endogenous peroxidase activity. Following, the sections were incubated with Glis2 (anti-goat, 1:50, Santa Cruz) overnight at 4 °C and secondary antibody at 37 °C for 2 h. After the sections were color-reacted with 0.02 % diaminobenzidine tetrahydrochloride (DAB) and washed with PBS, they were air-dried, dehydrated, cover slipped, and examined with Leica microscope (Leica, DM 5000B; Leica CTR 5000; Germany).

For immunofluorescent staining, sections were blocked with 10 % normal serum blocking solution species, containing 3 % (w/v) bovine serum albumin (BSA), 0.05 % Tween-20, and 0.1 % Triton X-100 for 2 h at room temperature to avoid unspecific staining. Then, the sections were incubated with primary antibodies against Glis2 (anti-goat, 1:50, Santa Cruz), NeuN (a marker of neuron, 1:200; Chemicon), GFAP (a marker of astrocytes, 1:200; Sigma), CD11b (a marker of microglia, 1:200; Sigma), and cleaved caspase-3 (a marker of apoptosis, 1:200; Invitrogen). They were incubated with all primary antibodies overnight at 4 °C, followed by a mixture of FITC- and TRITC-conjugated secondary antibodies for 2 h at room temperature. After washing with PBS 3 times for 10 min each, the sections were examined using Leica microscope.

Quantitative Analysis

Cell quantification was performed according to the principles described by (Koep et al. 1970). Cells double-labeled for Glis2 and phenotypic markers used in the experiment were counted. To identify the proportion of each phenotype-specific marker-positive cell expressing Glis2, a minimum of 200 phenotype-specific marker-positive cells were counted in adjacent to the wound in each section. Three adjacent sections per animal were sampled.

Statistical Analysis

All data in this paper were analyzed with Stata 7.0 statistical software (Systat Software Inc., San Jose, CA, USA). All values were expressed as mean ± SEM. The statistical analysis was performed by one-way analysis of variance (ANOVA) followed by Tukey's multiple comparison test.

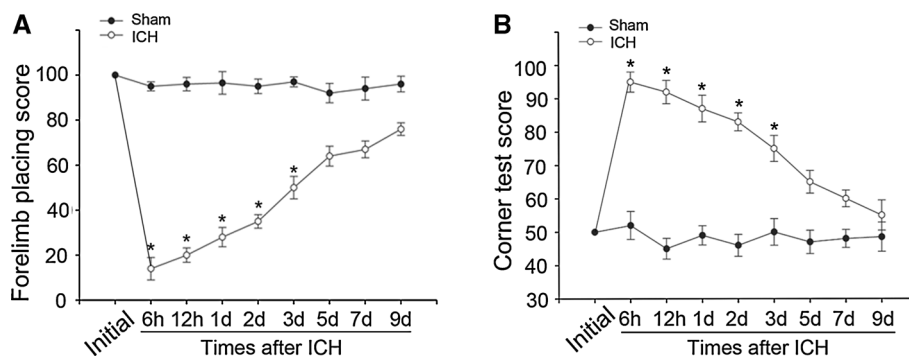


Fig. 1 Assessment and scores of behavioral tests at different time points on rats suffering from ICH. Forelimb placing (a) and corner turn testing scores (b) showed that the ICH group exhibited remarkable deficits compared with the sham-operated group over

the first 5 days ($*p < 0.05$, significantly different from the sham-operated group), with no significant difference at baseline or 5 days later

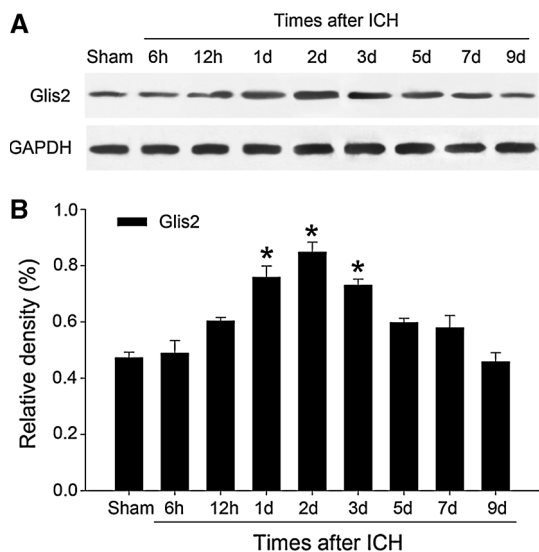


Fig. 2 Expression profiles of Glis2 around the hematoma at each time point after ICH by Western blot analysis. Glis2 was relatively low in the sham-controlled group, but increased gradually after ICH, peaked at day 2 and reduced thereafter (a). The bar graph indicated the relative density of Glis2 versus GAPDH at each time point (b). The data are mean \pm SEM. ($*p < 0.05$, significantly distinct from the sham group)

Statistical significance was defined as $p < 0.05$. Each experiment consisted of at least three replicates per condition.

Results

Functional Damage Assessed by Behavioral Tests at Diverse Time Points Following ICH

According to previous reports (Hua et al. 2002), a series of behavior tests were applied to evaluate acute and chronic

changes in sensorimotor function and plasticity in ICH rat model. In this study, forelimb placing and corner turn tests were employed. As shown in Fig. 1, the ICH group was obviously worse impaired when compared with the sham-operated group over the first 5 days ($*p < 0.05$). By 7 days and thereafter, neurological test scores of the rats went back to baseline.

Expression of Glis2 Increased After ICH

We performed Western blot to investigate the temporal expression patterns of Glis2 around the hematoma at different time points. As shown in the result, the Glis2 protein level was relatively low in the sham-operated group, progressively increased from 6 h after ICH, reached the peak at day 2, and then gradually returned to baseline (Fig. 2a, b). By the way, we also detected Glis2 protein expression in the contralateral brain, but failed to find any significant fluctuations (data not shown).

To further identify the variation and distribution of Glis2 after ICH, we performed immunohistochemistry staining on transverse cryosections of brain tissues at 2 days after ICH. Apparently, the number and intensity of Glis2-positive cells was extensively increased surrounding the hematoma (Fig. 3e, f), compared with the contralateral (Fig. 3c, d) and the sham group (Fig. 3a, b). Quantitative analysis documented the dramatic elevation of Glis2-positive cells after ICH around hematoma (Fig. 3g; $*p < 0.05$). These changes were compatible with the results from Western blot and suggested relevant biological functions of Glis2 after ICH.

Glis2 Located in the Neurons in the ICH Model

To further identify the cell types in the brain that expressed Glis2, double immunofluorescent staining was employed. We incubated Glis2 with different cell-specific markers,

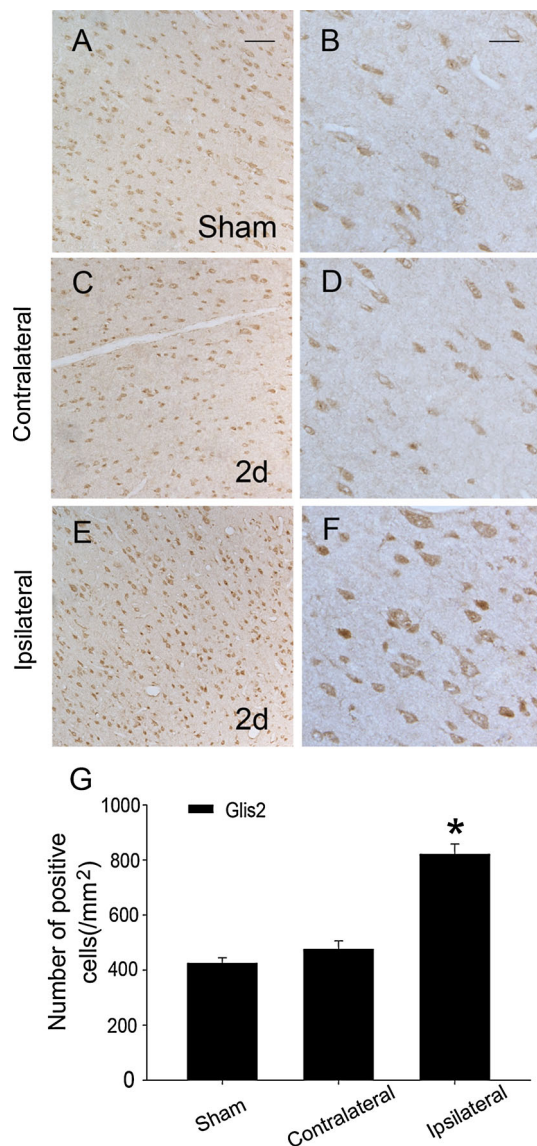


Fig. 3 Representative microphotographs for Glis2 immunohistochemistry in the rat brain surrounding the hematoma. Low level of Glis2 was detected in the sham-operated group (a, b). At 2 days after ICH, the contralateral group showed no significant difference in Glis2 expression (c, d), while the Glis2-positive cells in the ipsilateral group were greatly increased (e, f). **g** Quantitative analysis of Glis2-positive cells in the rat brain in the three groups. (* $p < 0.05$, significantly distinct from the sham-operated and contralateral groups) Scale bar left column 100 μm ; right column 50 μm

including NeuN, GFAP, and CD11b which represent neurons, astrocytes, and microglia, respectively. Microscopy indicated that Glis2 was specifically expressed in neurons (Fig. 4c, d), but not in astrocytes (Fig. 4g, h) or microglia (Fig. 4k, l). Glis2 was not expressed in the negative control (Fig. 4m, n). To identify the proportion of neurons expressing Glis2, at least 200 phenotype-specific marker-positive cells were counted for sham-controlled group and 2 days after ICH. Quantitative analysis reflected that Glis2 was highly increased in neurons (Fig. 4o).

Glis2 was Related to Neuronal Apoptosis after ICH

Since multiple studies have provided that neuronal apoptosis was a significant event surrounding hematoma in ICH (Sun et al. 2013; Xi et al. 2006) and the changes of Glis2 were mainly in neurons, it was reasonable for us to investigate whether Glis2 was involved in neuronal apoptosis. Then, we examined the expression profiles of active caspase-3 (a marker of apoptosis). As shown in the results, the expression of active caspase-3 increased after ICH, peaked at day 2, which was relevant with the expression of Glis2 in a time-dependent manner (Fig. 5a, b). In addition, immunofluorescent labeling showed that Glis2 co-localized well with active caspase-3 in neurons (Fig. 5e). As previous studies have demonstrated that Glis2 expression could affect the levels of Bcl-2 family members (Kim et al. 2008), Glis2 might also have regulatory functions on these genes after ICH. To further detect the association between Glis2 and neuronal apoptosis, we examined the expression profiles of Bax and Bcl-2. As shown in Fig. 5c, d, Bax was up-regulated and the expression was also parallel with that of Glis2 after ICH. Bcl-2 was reduced, which was opposite with those of Glis2 and Bax. These results reflected that Glis2 might participate in the process of neuronal apoptosis after ICH.

Glis2 Regulated Neuronal Apoptosis In Vitro

To further explore the exact role of Glis2 in neuronal apoptosis, hemin-induced apoptosis model in PC12 cells was built as described (Li et al. 2013). We incubated PC12 cells with 100 $\mu\text{mol/L}$ hemin at different time points and found the concomitant up-regulation of Glis2, active caspase-3, and Bax and down-regulation of Bcl-2 in a time-dependent way (Fig. 6a, b). What's more, siRNA was employed to knock down Glis2 in PC12 cells. Knocking down of Glis2 reduced the expression of active caspase-3 and Bax and specifically resulted in up-regulation of Bcl-2 with or without hemin stimulation (Fig. 6c, d). Additionally, immunofluorescent staining of PC12 cells also revealed that Glis2 silencing reduced the expression of active caspase-3 and nuclear condensation of these cells after hemin treatment (Fig. 7). These experiments all demonstrated that Glis2 was involved in neuronal pro-apoptosis function following ICH and mitochondria-mediated apoptotic pathway might be involved.

Discussion

ICH is a fierce and devastating CNS disease with high morbidity and mortality. Basal ganglia are one of the most common sites where human ICH often takes place

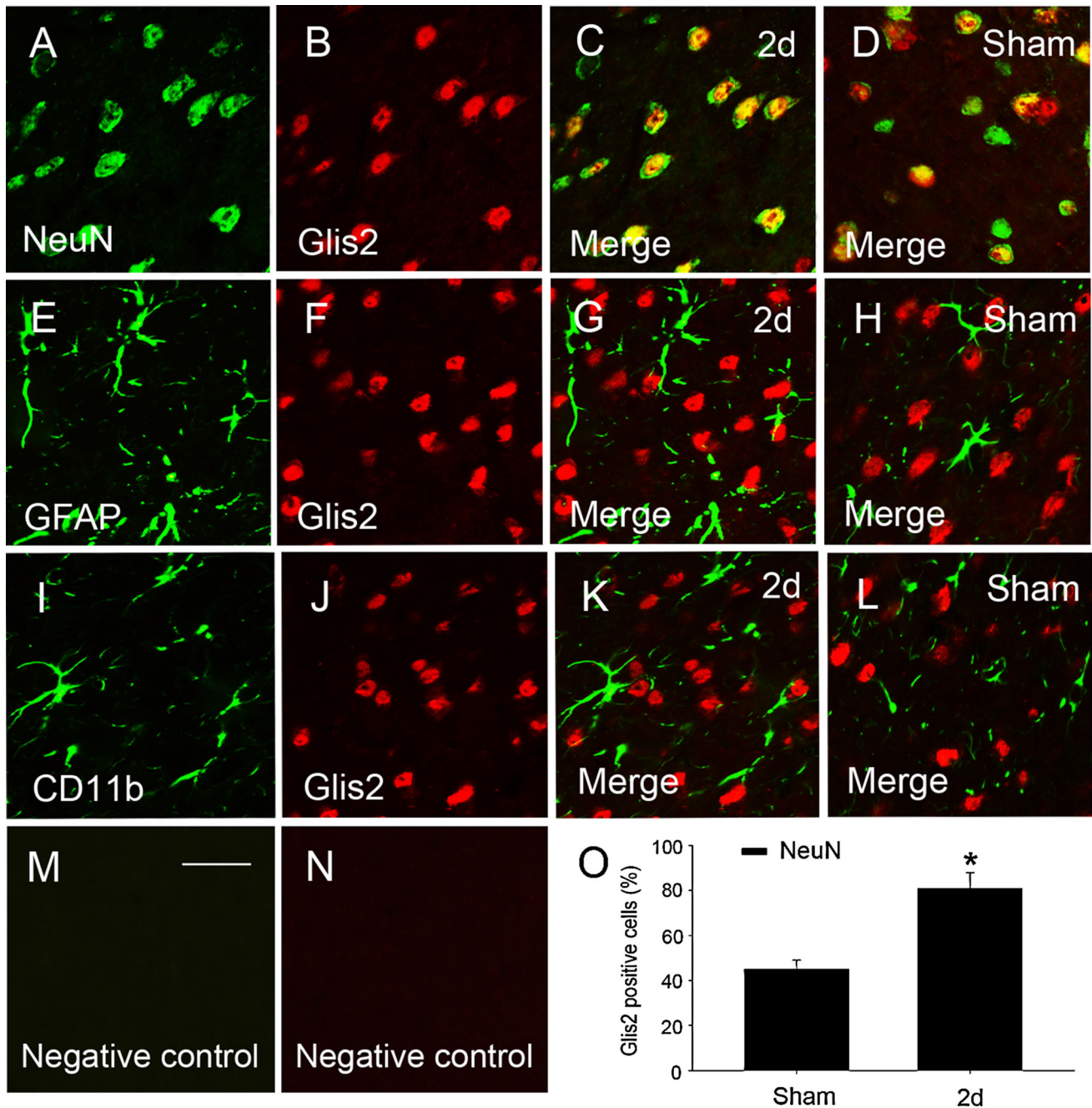


Fig. 4 Double immunofluorescence staining for Glis2 with different phenotype-specific markers in rat brain around hematoma. *Horizontal sections* were labeled with Glis2 (red, **b**, **f**, **j**) and different cell markers, including neuron marker (green, **a**, NeuN), astrocyte marker (green, **e**, GFAP), and microglia marker (green, **i**, CD11b). The yellow color in the merged images represented co-localization of

Glis2 with different phenotype-specific markers (**c**, **d**, **g**, **h**, **k**, **l**). Neurons marked by NeuN specifically contain Glis2 (**c**, **d**). No positive signal was found in the negative control (**m**, **n**). **o** Quantitative analysis of NeuN-positive cells expressing Glis2 (%) in the sham group and 2 days after ICH. (* $p < 0.05$, significant difference of ICH group compared with the sham) Scale bar: 50 μm (**a**–**n**)

(Naidech et al. 2010). In the present study, we imitated clinical ICH by injecting 50 μL autologous blood into the right basal ganglia of rats according to the corresponding hemorrhagic volume clinically (Yang et al. 2008). The rats suffering from ICH exhibited significantly functional damages assessed by behavioral tests. Western blot

analysis and immunohistochemistry revealed that Glis2 was significantly up-regulated surrounding the hematoma after ICH; meanwhile, there was a concomitant increase of active caspase-3 and Bax and down-regulation of Bcl-2. High level of Glis2 was found to be expressed in neurons around the hematoma and appeared to co-localize well with

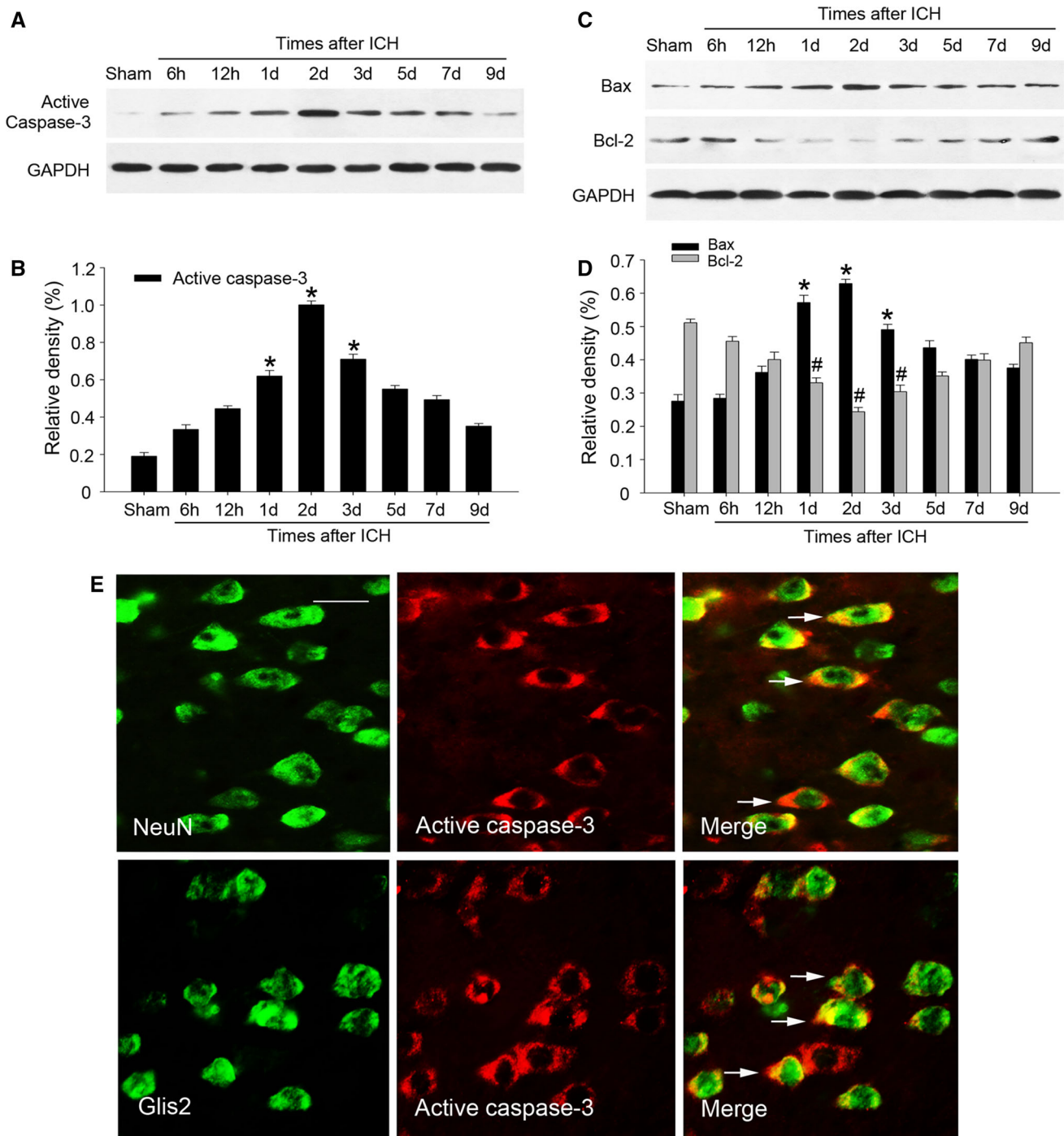


Fig. 5 Correlations of Glis2 with cell apoptosis following ICH. The expression of active caspase-3 and Bax increased, peaked at day 2 following ICH (a, c). The expression of Bcl-2 decreased after ICH and reached valley at 2 days (c). The bar graphs indicated the relative density of active caspase-3, Bax, and Bcl-2 versus GAPDH at each

time point (b, d). Data are presented as mean ± SEM. (*, # $p < 0.05$, significantly distinct from the sham group). Immunofluorescent staining showed co-staining of NeuN (green) and Glis2 (green) with active caspase-3 (red) in rat brain around hematoma (e). Scale bar 25 μm (e)

active caspase-3. Moreover, in vitro studies, depletion of Glis2 by siRNA reduced the expression of active caspase-3 and Bax and increased the expression of Bcl-2 in PC12 cells. Based on the data, we speculated that Glis2 might exert pro-apoptotic function in neurons after ICH.

In addition to the primary damage, ICH gives rise to a series of molecular and cellular events. Astrocyte proliferation, microglia activation, oligodendrocyte death, and neuronal apoptosis all have been implicated in the above processes (Wu et al. 2008; Bradl and Lassmann 2010;

Fig. 6 Modulation of Glis2 on cell apoptosis in vitro. PC12 cells were incubated with hemin at 100 $\mu\text{mol/L}$ for different times. Glis2, active caspase-3, and Bax were up-regulated, peaked at 12 h, while Bcl-2 had the opposite regulation (a). The bar graph indicated the relative density of Glis2, active caspase-3, Bax, and Bcl-2 versus GAPDH at each time point (b). The data are mean \pm SEM (*, ^, #, & $p < 0.05$, significantly different from the control group). The knockdown of Glis2 induced decreasing levels of active caspase-3 and Bax and had down-regulation of Bcl-2 expression (c). The bar graph indicated the relative density of Glis2, active caspase-3, Bax, and Bcl-2 versus GAPDH (d). Data are presented as mean \pm SEM. (*, ^, #, & $p < 0.05$, significantly different from the control-siRNA-treated group)

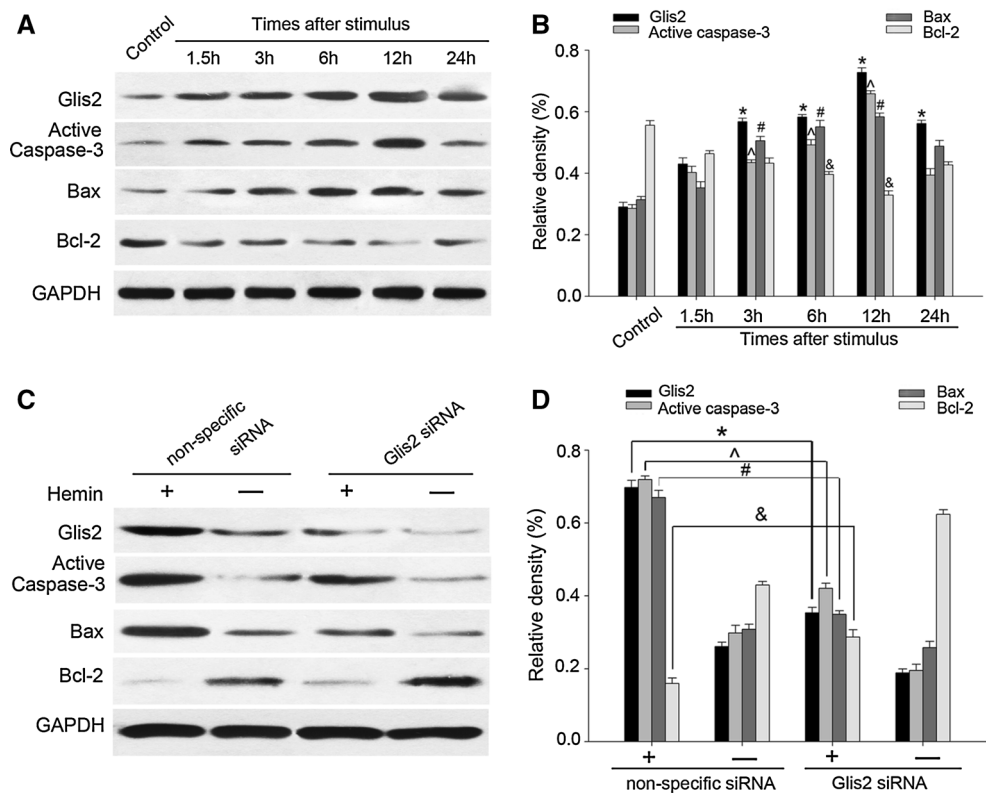
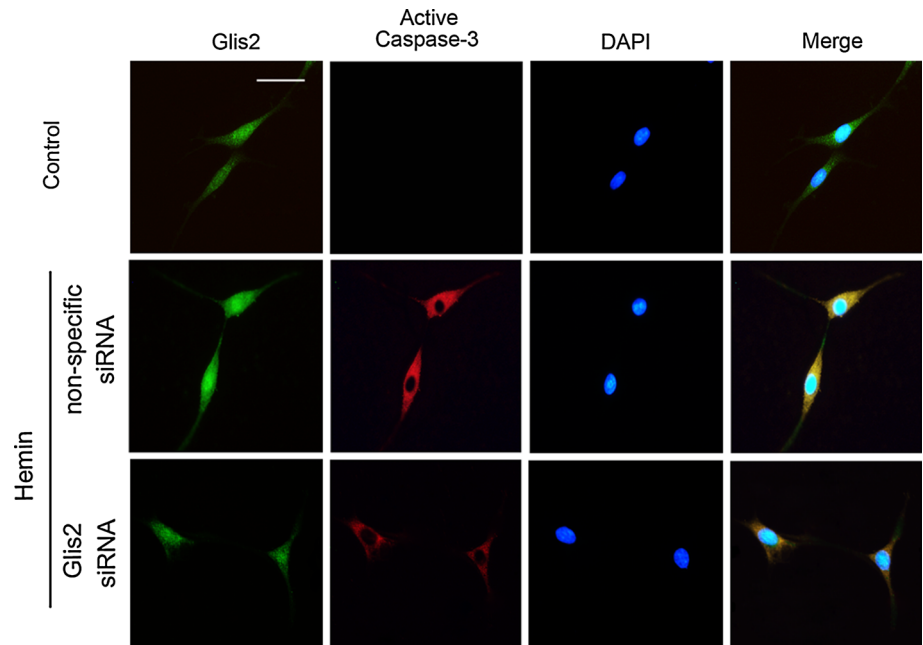


Fig. 7 Immunofluorescent staining showed the relationship of Glis2 and PC12 cell apoptosis. Compared with the control group, active caspase-3 and nuclei condensation were observed in PC12 cells at 12 h after the stimulation of hemin, but when Glis2 siRNA was used, these changes were reduced. The yellow color in the merged images represented colocalization of Glis2 (green) with active caspase-3 (red). Scale bars 50 μm



Matsushita et al. 2000). Among them, neuronal apoptosis is one of the most severe consequences, and mitochondria-mediated apoptosis pathway plays an important role in the process. Mitochondria are cellular organelles where soluble proteins including cytochrome c exist. Once induced, numerous neurotoxic factors lead to compromised integrity

of the mitochondrial outer membrane (OMM) which is called mitochondrial outer membrane permeabilization (MOMP) (Vaux 2011). Bcl-2 family proteins are the vital effectors of MOMP, during which the multi-domain proapoptotic proteins such as Bax and Bak oligomerize insert into the OMM, form lipidic pores wide enough to pass

cytochrome c, and lead to subsequent caspase-3 activation and cell apoptosis (Martinou and Youle 2011). However, the anti-apoptotic Bcl-2 protein has the possibility to directly interact with the BH3-only domain of Bax or Bak during the process of their oligomerization and thus represent an anti-apoptotic role (Xiong et al. 2014). Undoubtedly, the increase of the proportion of Bax/Bcl-2 facilitates additional release of cytochrome c and cell apoptosis. In this study, we found that the expression profiles of active caspase-3 and Bax were increased and Bcl-2 was down-regulated in the ICH model, which were similar to previous studies (Ke et al. 2013; Yuan et al. 2014).

Gli-similar (Glis) 1–3 form a subfamily of Krüppel-like zinc finger proteins that are related to members of the Gli and Zic subfamilies. Members of these families share a highly conserved tandem repeat of five C2H2-type zinc finger (ZF1–ZF5) motifs. These zinc finger domains recognize specific DNA elements, referred to as Gli-binding sites (GBS), in the promoter regions of target genes and can regulate their transcription in a positive or negative manner (Kang et al. 2010). Glis1–3 play critical roles in the regulation of a number of physiological processes and have been implicated in several pathologies. Increased expression of Glis1 promotes certain aspects of epidermal differentiation and may have a role in psoriasis (Kang et al. 2010). Glis2 and Glis3 proteins have been demonstrated to localize to the primary cilium, a signaling organelle that has been implicated in several pathologies, including cystic renal diseases. Results from Attanasio M described that Glis2 was mutated in nephronophthisis and presented essential role for the maintenance of renal tissue architecture through the prevention of apoptosis and fibrosis (Attanasio et al. 2007). Glis2 is also expressed in the neurons (Hosking et al. 2007), but its definite function has not been fully explored. In the present study, we found that Glis2 was significantly increased in perihematomal region in adult rats after ICH (Figs. 2, 3). Immunofluorescence indicated that Glis2 was expressed in neurons (Fig. 4). Based on these, we suspected that Glis2 might be associated with neuronal biological function changes following ICH. Subsequently, we found that the increase of Glis2 was relevant with the up-regulation of active caspase-3 and Bax and down-regulation of Bcl-2 (Fig. 5). Moreover, Glis2 was localized well with active caspase-3 in the neurons (Fig. 5). Thus, we speculated that Glis2 might participate in neuronal apoptosis after ICH. In order to confirm our suspicion, we employed hemin-induced cell apoptosis model in PC12 cells. Active caspase-3 and Bax were always parallel with Glis2, while Bcl-2 had an opposite expression (Fig. 6). Decreasing Glis2 levels by RNA-interference in PC12 cells reduced active caspase-3 and Bax but induced up-regulation of Bcl-2 (Figs. 6, 7). Based

on the results, Glis2 might exert pro-apoptosis function in neurons following ICH and mitochondria-mediated apoptotic pathway might be involved. This result was inconsistent with the finds of Attanasio et al. as described above (Attanasio et al. 2007); thus, the different roles of Glis2 in the pro- or anti-apoptosis seemed to be tissue- or disease-specific.

In conclusion, the present research for the first time detected the expression and variation of Glis2 surrounding the hematoma, and all the data certificated the involvement of Glis2 in neuronal apoptosis following ICH. Nevertheless, further studies remain to be done to seek the underlying cellular and molecular mechanisms and therapeutic potentials of Glis2 for ICH. Thereby, we can achieve better prognosis for patients suffering from ICH as well as ischemic stroke and other neurodegenerative diseases.

Acknowledgments This work was supported by National Natural Science Foundation of China (No. 81371299); Technology Innovation Programme of Jiangsu province (YKC13075, YKC13086).

Conflict of interest The authors declare no conflict of interest.

References

- Aronowski J, Zhao X (2011) Molecular pathophysiology of cerebral hemorrhage: secondary brain injury. *Stroke* 42(6):1781–1786
- Attanasio M, Uhlenhaut NH, Sousa VH, O'Toole JF, Otto E, Anlag K, Klugmann C, Treier AC, Helou J, Sayer JA, Seelow D, Nurnberg G, Becker C, Chudley AE, Nurnberg P, Hildebrandt F, Treier M (2007) Loss of GLIS2 causes nephronophthisis in humans and mice by increased apoptosis and fibrosis. *Nat Genet* 39(8):1018–1024
- Bradl M, Lassmann H (2010) Oligodendrocytes: biology and pathology. *Acta Neuropathol* 119(1):37–53
- Cregan SP, MacLaurin JG, Craig CG, Robertson GS, Nicholson DW, Park DS, Slack RS (1999) Bax-dependent caspase-3 activation is a key determinant in p53-induced apoptosis in neurons. *J Neurosci* 19(18):7860–7869
- Elmore S (2007) Apoptosis: a review of programmed cell death. *Toxicol Pathol* 35(4):495–516
- Hosking CR, Ulloa F, Hogan C, Ferber EC, Figueroa A, Gevaert K, Birchmeier W, Briscoe J, Fujita Y (2007) The transcriptional repressor Glis2 is a novel binding partner for p120 catenin. *Mol Biol Cell* 18(5):1918–1927
- Hua Y, Schallert T, Keep RF, Wu J, Hoff JT, Xi G (2002) Behavioral tests after intracerebral hemorrhage in the rat. *Stroke* 33(10):2478–2484
- Hwang BY, Appelboom G, Ayer A, Kellner CP, Kotchetkov IS, Gigante PR, Haque R, Kellner M, Connolly ES (2011) Advances in neuroprotective strategies: potential therapies for intracerebral hemorrhage. *Cerebrovasc Dis* 31(3):211–222
- Ikram MA, Wieberdink RG, Koudstaal PJ (2012) International epidemiology of intracerebral hemorrhage. *Curr Atheroscler Rep* 14(4):300–306
- Kang HS, ZeRuth G, Lichti-Kaiser K, Vasanth S, Yin Z, Kim YS, Jetten AM (2010) Gli-similar (Glis) Kruppel-like zinc finger proteins: insights into their physiological functions and critical roles in neonatal diabetes and cystic renal disease. *Histol Histopathol* 25(11):1481–1496

- Karabiyikoglu M, Hua Y, Keep RF, Ennis SR, Xi G (2004) Intracerebral hirudin injection attenuates ischemic damage and neurologic deficits without altering local cerebral blood flow. *J Cereb Blood Flow Metab* 24(2):159–166
- Ke K, Li L, Rui Y, Zheng H, Tan X, Xu W, Cao J, Xu J, Cui G, Xu G, Cao M (2013) Increased expression of small heat shock protein alphaB-crystallin after intracerebral hemorrhage in adult rats. *J Mol Neurosci* 51(1):159–169
- Keep RF, Hua Y, Xi G (2012) Intracerebral haemorrhage: mechanisms of injury and therapeutic targets. *Lancet Neurol* 11(8):720–731
- Kim YS, Kang HS, Herbert R, Beak JY, Collins JB, Grissom SF, Jetten AM (2008) Kruppel-like zinc finger protein Glis2 is essential for the maintenance of normal renal functions. *Mol Cell Biol* 28(7):2358–2367
- Koep LJ, Konigsmark BW, Sperber EE (1970) Cellular changes in the human supraoptic and paraventricular hypothalamic nuclei in dehydration. *J Neuropathol Exp Neurol* 29(2):254–265
- Li L, Ke K, Tan X, Xu W, Shen J, Zhai T, Xu L, Rui Y, Zheng H, Zhai P, Zhao J, Cao M (2013) Up-regulation of NFATc4 involves in neuronal apoptosis following intracerebral hemorrhage. *Cell Mol Neurobiol* 33(7):893–905
- Martinou JC, Youle RJ (2011) Mitochondria in apoptosis: Bcl-2 family members and mitochondrial dynamics. *Dev Cell* 21(1):92–101
- Matsushita K, Meng W, Wang X, Asahi M, Asahi K, Moskowitz MA, Lo EH (2000) Evidence for apoptosis after intercerebral hemorrhage in rat striatum. *J Cereb Blood Flow Metab* 20(2):396–404
- Naidech AM, Bernstein RA, Alberts MJ, Bleck TP (2010) Prior antiplatelet use does not affect hemorrhage growth or outcome after ICH 2. *Neurology* 74(6):526–527
- Plesnila N, von Baumgarten L, Retiounskaia M, Engel D, Ardeshiri A, Zimmermann R, Hoffmann F, Landshamer S, Wagner E, Culmsee C (2007) Delayed neuronal death after brain trauma involves p53-dependent inhibition of NF-kappaB transcriptional activity. *Cell Death Differ* 14(8):1529–1541
- Sun H, Li L, Zhou F, Zhu L, Ke K, Tan X, Xu W, Rui Y, Zheng H, Zhou Z, Yang H (2013) The member of high temperature requirement family HtrA2 participates in neuronal apoptosis after intracerebral hemorrhage in adult rats. *J Mol Histol* 44(4):369–379
- Vasanth S, ZeRuth G, Kang HS, Jetten AM (2011) Identification of nuclear localization, DNA binding, and transactivating mechanisms of Kruppel-like zinc finger protein Gli-similar 2 (Glis2). *J Biol Chem* 286(6):4749–4759
- Vaux DL (2011) Apoptogenic factors released from mitochondria. *Biochim Biophys Acta* 1813(4):546–550
- Villavicencio EH, Walterhouse DO, Iannaccone PM (2000) The sonic hedgehog-patched-gli pathway in human development and disease. *Am J Hum Genet* 67(5):1047–1054
- Wu J, Yang S, Xi G, Song S, Fu G, Keep RF, Hua Y (2008) Microglial activation and brain injury after intracerebral hemorrhage. *Acta Neurochir Suppl* 105:59–65
- Wu X, Jin W, Liu X, Fu H, Gong P, Xu J, Cui G, Ni Y, Ke K, Gao Z, Gao Y (2012) Cyclic AMP response element modulator-1 (CREM-1) involves in neuronal apoptosis after traumatic brain injury. *J Mol Neurosci* 47(2):357–367
- Xi G, Keep RF, Hoff JT (2006) Mechanisms of brain injury after intracerebral haemorrhage. *Lancet Neurol* 5(1):53–63
- Xiong S, Mu T, Wang G, Jiang X (2014) Mitochondria-mediated apoptosis in mammals. *Protein Cell* 5:737–749
- Yang S, Song S, Hua Y, Nakamura T, Keep RF, Xi G (2008) Effects of thrombin on neurogenesis after intracerebral hemorrhage. *Stroke* 39(7):2079–2084
- Yuan D, Shen J, Yan Y, Wu X, Li A, Guo A, Wu Y, Duan C, Tang C, Zhang D, Ji Y (2014) Upregulated expression of SSTR1 is involved in neuronal apoptosis and is coupled to the reduction of bcl-2 following intracerebral hemorrhage in adult rats. *Cell Mol Neurobiol* 34:951–961
- Zhang F, Jetten AM (2001) Genomic structure of the gene encoding the human GLI-related, Kruppel-like zinc finger protein GLIS2. *Gene* 280(1–2):49–57
- Zhang F, Nakanishi G, Kurebayashi S, Yoshino K, Perantoni A, Kim YS, Jetten AM (2002) Characterization of Glis2, a novel gene encoding a Gli-related, Kruppel-like transcription factor with transactivation and repressor functions. Roles in kidney development and neurogenesis. *J Biol Chem* 277(12):10139–10149